Nonlinear Model Predictive Control of the Hydraulic Fracturing Process

Kuan-Han Lin, John P. Eason,
Zhou (Joyce) Yu, Lorenz T. Biegler

Department of Chemical Engineering, Carnegie Mellon University,
Pittsburgh, PA 15213 USA
(e-mail: kuanhanl, jeason, zhouy1, lb01@andrew.cmu.edu)

Abstract: Hydraulic fracturing has drawn significant attention over the past decade, as it can recover crude oil and natural gas from shale deposits previously considered inaccessible, which brings considerable economic benefits. However, hazardous operating conditions of extremely high pressure and environmental concerns require us to control this process carefully. Unfortunately, nonhomogeneous rock properties make this process difficult to control. Therefore, an accurate dynamic model and a well-designed controller are needed. In this work, we use the well-known Perkins-Kern-Nordgren (PKN) model with reformulation to solve the moving boundary problem. Next, the process is controlled by a standard Nonlinear Model Predictive Controller (NMPC) and multistage NMPC. We find that the process performance deteriorates under the influence of uncertainty with standard NMPC. When we control the process with standard NMPC, the pressure violation happens in one of the parameter mismatch cases. Nonetheless, when we apply multistage NMPC and consider the uncertainty evolution with a scenario tree, no constraint violations occur for all cases for both time-invariant and time-varying uncertainties. We also discuss the computational performance of different robust horizons for multistage NMPC. Our results demonstrate that the multistage NMPC is a promising approach to handle uncertainty caused by nonhomogeneous rock properties in the hydraulic fracturing process.

Keywords: Model Predictive and Optimization-based Control, Hydraulic Fracturing, Dynamic Optimization, Optimal Control, Robust Nonlinear Model Predictive Control.

1. INTRODUCTION

The goal of hydraulic fracturing is to enhance the production of a stimulated well. The process starts with perforation to create initial fracture paths along a well. Then, high-pressure fracturing fluid, consisting of water, chemical additives, and proppant, is pumped down a wellbore for further fracture propagation. After the end of pumping, the proppant will be trapped by the closing fracture walls, creating a fracture volume. The created fracture volume stimulates the extra flow of hydrocarbons that geologists once believed were inaccessible. This highly increasing production can yield great economic benefits. However, there are some issues in this process. First, the fracking fluid contains toxic chemicals that could contaminate groundwater if fractures connect to aquifer systems. More importantly, if the pressure becomes too high during pumping, the pumps may be destroyed and severe damage would occur in the rock formation. These problems demand that the process be controlled carefully and accurately. However, rock properties may be nonhomogeneous, which makes it hard to control the growth of the fracture.

A traditional control strategy of hydraulic fracturing (Gu and Hoo, 2015) is primarily an open-loop process that starts with a shorter and smaller scale test (called a mini-frac) and then applies the obtained information to execute the offline optimization to determine flow rates and concentrations of materials for the entire procedure, before the main fracturing process. However, this strategy is suboptimal since it does not use feedback with real time measurements from the process. Gu and Hoo (2015) consider a closed-loop process that uses the measured data to update the inputs when the main fracturing process proceeds. The feedback control is achieved by applying a Quadratic Dynamic Matrix Control (QDMC) controller, which performs better than the traditional open-loop controller. Siddhamshetty et al. (2018) implement Model Predictive Control (MPC) for the design of the feedback control to achieve the required proppant concentration across the fracture at the end of pumping. Nonetheless, these two haven't considered the uncertain parameters such as rock properties in the process. Singh Sidhu et al. (2018) propose an approximate dynamic programming (ADP) based approach for the closed-loop control to deal with the uncertainties. Yet the drawback of this approach is that a pre-solved suboptimal control policy is needed beforehand, which makes it hard to implement in the real world. Also, the pressure constraint, which is one of the most important safety concerns in the managed pressure drilling process (Bellout et al., 2012), is not considered in these references.

In order to have good control performance of the hydraulic fracturing process with appropriate constraints,

Model Predictive Control (MPC) is applied to this process. MPC is widely applied due to its effectiveness in handling constraints and multiple-input-multiple-output (MIMO) systems (Qin and Badgwell, 2003). Its nonlinear version, Nonlinear Model Predictive Control (NMPC) solves a Nonlinear Programming (NLP) problem to minimize the objective function within a finite horizon subject to constraints. However, standard NMPC is sensitive to plant-controller mismatch. Some uncertainties in the process are likely to deteriorate the performance of standard NMPC, causing safety hazards or machine damage. A few references use the ensemble Kalman filter (EnKF) to infer these uncertainties from measurements, assuming known mean and covariance (Jafarpour and McLaughlin, 2009) (Narasingam et al., 2018). Without requiring this assumption, a robust NMPC called multistage NMPC (Lucia et al., 2013) is implemented to cope with these uncertainties. Multistage NMPC has already been applied to some practical problems such as CSTR and semi-batch reactor (Yu and Biegler, 2019) (Holtorf et al., 2019). The main idea of multistage NMPC is to represent the possible uncertainty evolution by building a scenario tree structure. Therefore, as new information is available at the next time step, the next control input can be adjusted based on this new information to counteract the influence of the uncertainties.

The paper is organized as follows. In Section 2 we introduce the Perkins-Kern-Nordgren (PKN) model that we use to model the fracturing process; in Section 3 we present the overview of standard NMPC and formulate the framework of multistage NMPC; Section 4 presents the result of applying standard NMPC and multistage NMPC to hydraulic fracturing process. Finally, Section 5 provides conclusions and future perspectives.

2. HYDRAULIC FRACTURING MODEL

In this work, a well-known fracturing model called Perkins-Kern-Nordgren (PKN) model (Nordgren, 1972)(Perkins and Kern, 1961) is built for fracture propagation. This model has been mainly used in shale formations especially for the Sneddon-type rock (Daemen and Schultz, 1995). We consider the following assumptions:

(1) The stresses above and below the pay zone are sufficiently large that the fracture is restricted within a horizontal rock layer. Namely, the fracture propagates at a fixed height as depicted in Fig. 1.
(2) The fracture propagates unidirectionally in the rock layer.
(3) The fracture length is much greater than the fracture width.
(4) The cross section of the fracture is elliptical and the maximum width of fracture is proportional to the net pressure.
(5) The fracturing fluid is Newtonian fluid and perfectly mixed.

The governing equations of PKN model can be formulated by adopting the fundamental principles of local fluid mass balance equation (1) and the global fluid mass balance equation (2):
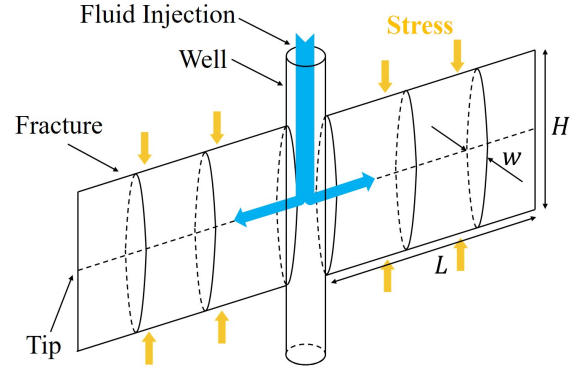
Fig. 1. PKN hydraulic fracture

$$\frac{\partial q}{\partial x} + u + \frac{\partial A}{\partial t} = 0 \tag{1}$$

$$q_{leakoff} + q_{storage} = q_{total} \tag{2}$$

where q is the flowrate in the fracture, u is the flowrate of leakoff per unit length, and A is the cross-sectional area of the fracture. The three terms in equation (1) denote the net flow change, the amount of leakoff, and the fracture volume change of a small element in the fracture. The three terms in equation (2) indicate the total amount of leakoff, the total liquid stored in the fracture, and the total fluid pumped into the fracture. For simplicity, leakoff terms are ignored here. After some derivation shown in Detournay et al. (1990), Kovalyshen and Detournay (2010), and Nordgren (1972) and adding the pressure relation in equation (5) and (6), the hydraulic fracturing model can be written as follows with two initial conditions and two boundary conditions:

$$-\frac{E}{2\mu H\pi^3(1-\nu^2)}\frac{\partial^2 \bar{w}^4}{\partial x^2} + \frac{\partial \bar{w}}{\partial t} = 0 \tag{3}$$

$$\int_0^L \bar{w}\,dx = \frac{1}{H}\int_0^t q_f\,dt \tag{4}$$

$$P_{head} = \frac{E}{2H(1-\nu^2)}w + \sigma - \rho g H_{well} + P_{fr} \tag{5}$$

$$P_{fr} = \frac{16\mu q_f H_{well}}{\pi R^4} \tag{6}$$

$$\text{IC 1}: L(t=0) = 0, \qquad \text{IC 2}: \bar{w}(t=0,x) = 0 \tag{7}$$

$$\text{BC 1}: q(t,x=0) = q_f, \quad \text{BC 2}: \bar{w}(t,x=L) = 0 \tag{8}$$

where E and ν are Young's modulus and Poisson's ratio respectively, μ is the viscosity of fluid, H is the height of fracture, σ is the confining stress of the rock formation, ρ is the density of fluid, g is the gravity constant, H_{well} is the depth of the well, P_{fr} is the friction loss in the well, and R is the radius of the well. The control input is the pump rate q_f and the states are average width $\bar{w}$, length L of the fracture, and the wellhead pressure P_{head}.

Before applying NMPC to the process, we notice that the second boundary condition is related to one of the variables, L, which means this model is a moving boundary problem. In order to deal with this problem, a new coordinate θ is introduced and defined as follows (Detournay et al., 1990) (Kovalyshen and Detournay, 2010):

$$\theta = x/L(t), \quad \theta \in [0,1] \tag{9}$$

The advantage of this transformation is that a bounded coordinate can assign the second boundary condition at a specific position $\theta = 1$ instead of moving throughout the whole process. Coordinate conversion requires the following transformation of spatial and time derivatives:

$$\left.\frac{\partial}{\partial x}\right|_t = \frac{1}{L}\left.\frac{\partial}{\partial \theta}\right|_t \quad \text{and} \quad \left.\frac{\partial}{\partial t}\right|_x = \left.\frac{\partial}{\partial t}\right|_\theta - \frac{\theta}{L}\frac{dL}{dt}\left.\frac{\partial}{\partial \theta}\right|_t$$

After the transformation, Equations (3) and (4) become:

$$-\frac{E}{2\mu H \pi^3 (1-\nu^2)}\frac{1}{L^2}\frac{\partial^2 \bar{w}^4}{\partial \theta^2} + \frac{\partial \bar{w}}{\partial t} - \frac{\theta}{L}\frac{dL}{dt}\frac{\partial \bar{w}}{\partial \theta} = 0 \tag{10}$$

$$L\int_0^1 \bar{w}\, d\theta = \frac{1}{H}\int_0^t q_f\, dt \tag{11}$$

With Equations (10), (11), pressure relation (5), (6), initial conditions (7), and boundary conditions (8), we obtain the dynamic model of the hydraulic fracturing process.

3. NMPC FORMULATION

3.1 Standard NMPC

We consider a nonlinear dynamic system in the process with uncertainties:

$$z_{i+1} = f(z_i, u_i, d_i), \quad z_0 = x(k) \tag{12}$$

where $x(k) \in \mathbb{R}^{n_x}$ is the process states serving as the initial condition of the model, $z_i \in \mathbb{R}^{n_x}$, $u_i \in \mathbb{R}^{n_u}$ are the *predicted* states and controls, and $d_i \in \mathbb{R}^{n_d}$ denotes the uncertainty in the plant. This model can be introduced into a nonlinear optimization problem as equation (13), that strives to minimize an objective that quantifies either deviation from a set-point or an economic goal.

$$\min_{u_i, z_i} F(z_N) + \sum_{i=0}^{N-1} \psi(z_i, u_i)$$
$$\text{s.t. } z_{i+1} = f(z_i, u_i, \bar{d}_i), \quad i = k, ..., N-1 \tag{13}$$
$$z_k = x(k)$$
$$z_i \in \mathbb{X}, \, z_N \in \mathbb{X}_f, \, u_i \in \mathbb{U}$$

After solving the optimization problem (13), the optimal trajectory is obtained but only the first control input is introduced back into the process as in equation (12). At the next time step $k+1$ we read the new states to update the initial condition in the optimization problem. This procedure is repeated to keep updating the control input. Note that standard NMPC only takes the nominal value of d_i in the controller; it ignores the impact of uncertainty and doesn't provide the recourse to counteract it.

3.2 Multistage NMPC

The main idea of multistage NMPC is to model the uncertainty evolution by a scenario tree as shown in Fig. 2. A node denotes a state vector z_k in the scenario tree. Each path from the root node z_0 to one of the leaf nodes

is a scenario. The prediction horizon N_p is the number of stages considered in multistage NMPC. Starting from the first node corresponding to the current state $x(k)$, the branches from each node represent the maximum, nominal, and minimum value of the uncertainty d_l respectively with the corresponding control u_k. Therefore, three different states are predicted for the next step t_{k+1}. Then, for predicted states at t_{k+1}, the branching propagates with another three predicted states at t_{k+2}. For example in Fig. 2 there are 27 scenarios and a prediction horizon length of 3. Note that the scenario tree grows exponentially with the prediction horizon and the number of uncertainties, leading to an intractable multi-stage problem.
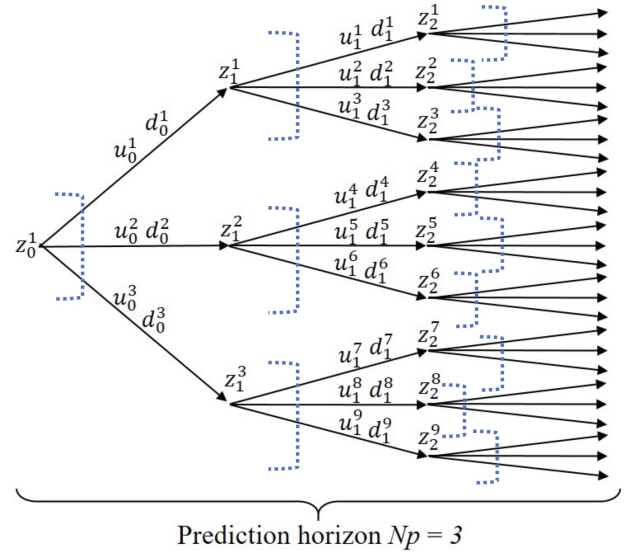
Fig. 2. Fully-branched scenario tree with nonanticipativity constraints (dotted brackets)

In order to handle this issue, we consider that the branching of scenario tree stops at a certain stage (called the robust horizon) and the uncertainty remains constant till the end of each scenario. For example, the truncated tree in Fig. 3 has 1 robust horizon and 3 scenarios. This simplification can be justified that the control inputs and state variables for the far future don't need to be calculated as accurately as the next stage because only the first step of the control profile is applied to the process, and the far future stages will be refined later as time moves forward.

Finally, important restrictions called non-anticipativity constraints (NAC) must also be applied to multistage NMPC. The NAC is needed because the decision variable at current stage cannot anticipate the realization of the uncertainty d_i in the future. Hence, all control inputs that branch from the same parent node must be equal to realize the real-time decision situation (i.e., $u_0^1 = u_0^2 = u_0^3$ in Fig. 3). Note that this constraint only applies within the robust horizon. Beyond the robust horizon, the control inputs are not constrained and they act as recourse variables to allow the system to recover from uncertainties. This improves the performance and decreases the conservativeness of the controller, which is the advantage of multistage NMPC.

The corresponding optimization problem for multistage NMPC with prediction horizon N can be defined by:
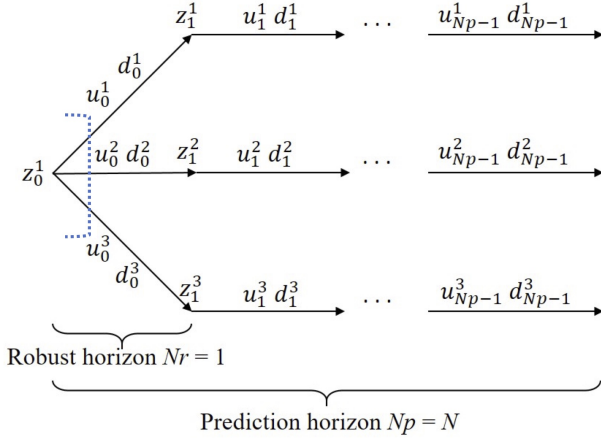
Fig. 3. Truncated scenario tree: $N_r = 1$

$$\min_{u_i, z_i} \sum_{c \in \mathbb{C}} w_c \left(F(z_N^c) + \sum_{i=0}^{N-1} \psi(z_i^c, u_i^c) \right)$$

$$\text{s.t. } z_{i+1}^c = f(z_i^c, u_i^c, d_i^c), \quad i = k, ..., N-1 \qquad (14a)$$

$$z_k^c = x(k) \qquad (14b)$$

$$u_i^c = u_i^{\bar{c}} \quad \text{if} \quad z_k^c = z_k^{\bar{c}}, \quad c, \bar{c} \in \mathbb{C} \qquad (14c)$$

$$z_i^c \in \mathbb{X}, \ z_N^c \in \mathbb{X}_f, \ u_i^c \in \mathbb{U} \qquad (14d)$$

where $\mathbb{C}$ denotes the set of scenarios and w_c represents the weight of the scenario c, coming from the historic data or probability distribution. The objective function of multistage NMPC considers the sum of the weighted scenario with stage cost $\psi(\cdot)$ and terminal cost $F(\cdot)$. Note that equation (14c) represents the non-anticipativity constraint.

4. SIMULATION RESULTS

With the hydraulic fracturing model, the NMPC problem is formulated to track a desired set-point for the pump rate q_f with an objective function considering the stage cost $\psi(\cdot)$ in equation (13) and (14) as follows:

$$min \quad \sum_{i=0}^{N-1} (q_{fi} - q^{SP})^2$$

The prediction horizon N_p is chosen to be 30 steps with sampling time $\Delta t = 2 \, min$. Therefore, the total simulation time is 60 minutes. The control input is the pump rate q_f and the states are average width $\bar{w}$, length L of the fracture, and the wellhead pressure P_{head} with two safety constraints listed in Table 1:

Table 1. State and control constraints

	Min.	Max.	Unit
P_{head}	-	6.34×10^7	Pa
$\frac{dq_f}{dt}$	-	0.795	m^3/min^2

The uncertain parameter considered here is the Young's modulus, which is one of the rock properties. We assume it can vary by $\pm 5\%$ with respect to its nominal value as shown in Table 2.

Table 2. Value of Young's modulus E (Pa)

deviation	value
-5%	2.28×10^{10}
Nominal	2.40×10^{10}
+5%	2.52×10^{10}

The simultaneous approach solves the NLP problem of NMPC (13) and (14). Equations (10) and (11) are discretized in space using finite differences with $\Delta \theta = 0.05$, and in time using an implicit Euler discretization with $\Delta t = 2 \, min$. This leads to the dynamic model (15):

$$-\frac{E}{2\mu H \pi^3 (1-\nu^2)} \frac{1}{L_i^2} \left(\frac{\bar{w}_{i,j+1}^4 - 2\bar{w}_{i,j}^4 + \bar{w}_{i,j-1}^4}{\Delta \theta^2} \right) +$$
$$\left(\frac{\bar{w}_{i,j} - \bar{w}_{i-1,j}}{\Delta t} \right) - \frac{\theta_j}{L_i} \left(\frac{L_i - L_{i-1}}{\Delta t} \right) \left(\frac{\bar{w}_{i,j} - \bar{w}_{i,j-1}}{\Delta \theta} \right) = 0 \qquad (15a)$$

$$L_i \sum_{j=1}^{M-1} \frac{\bar{w}_{i,j} + \bar{w}_{i,j+1}}{2} \Delta \theta = \frac{1}{H} \sum_{i=1}^{N-1} \frac{q_{fi} + q_{fi+1}}{2} \Delta t \qquad (15b)$$

$$P_{head,i} = \frac{E}{2H(1-\nu^2)} w_{i,1} + \sigma - \rho g H_{well} + \frac{16\mu q_{fi} H_{well}}{\pi R^4} \qquad (15c)$$

$$L_{i=1} = 0, \ \bar{w}_{i=1,j} = 0, \ q_{i,j=1} = q_{fi}, \ \bar{w}_{i,j=M} = 0 \qquad (15d)$$

$$i = 1, ..., N, \quad j = 1, ..., M \qquad (15e)$$

The discretized model is built in the optimization modeling platform Pyomo 5.6.6 (Hart et al., 2011) and solved by the nonlinear solver IPOPT 3.12 (Waechter and Biegler, 2006). All cases are run on a HPE-180t desktop running on Ubuntu 18.04.3 with an Intel Core i7-930 CPU, 2.8 GHz, and 8.8 GB RAM.

4.1 Performance comparison between standard NMPC and multistage NMPC

We first compare the performance between standard NMPC and multistage NMPC with time-invariant uncertainty. For standard NMPC cases, the Young's modulus E always stays at the nominal value in the controller and the Young's modulus in the process model is realized constantly with three different values respectively in each case. From Fig. 4a, the standard NMPC performs well without parameter mismatch. The pressure keeps increasing as more fluid is pumped into the fracture. When the pressure reaches the bound, the controller responds by decreasing the flowrate to avoid the pressure exceeding the bound. Since there is no mismatch between the controller and the process model, the standard NMPC makes the correct decisions and no constraint violations occur. However, this perfect case without parameter mismatch would rarely happen in the real world.

If the uncertainty parameter used in the control model differs from that of the process, infeasibilities may occur. In Fig. 4b, Young's modulus in the process is 5% less than that in the controller. The controller assumes that the pressure would exceed its bound, so it decreases the flowrate while the pressure remains in bound for the whole process. This case is still acceptable because no constraint violation occurs, despite the unexpected decrease of flowrate. On the other hand, for the case in
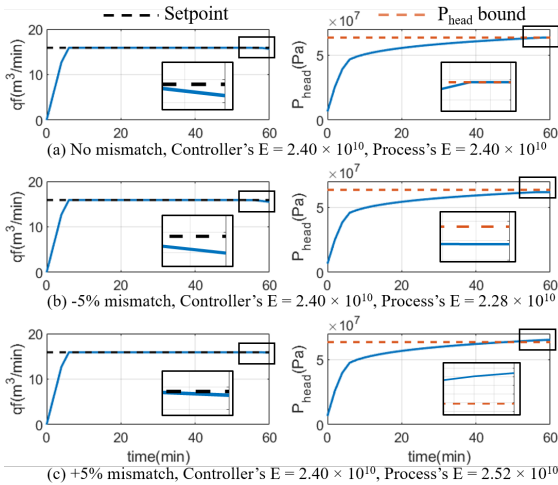
Fig. 4. Different uncertainty realization cases controlled by standard NMPC

Fig. 5. Different uncertainty realization cases controlled by multistage NMPC

Fig. 4c, Young's modulus in the process is 5% greater than that in the controller. The controller doesn't account for the pressure violation and cannot take a proper action accordingly. This result is unacceptable, and it may cause a costly emergency shutdown. Hence, we resort to multistage NMPC to solve this problem.

In order to handle the constraint violations, we apply multistage NMPC to the previous three cases, where the Young's modulus is set to be the nominal value, -5%, and +5% respectively. The robust horizon in multistage NMPC is considered to be $N_r = 1$ and thus the truncated scenario tree has 3 branching scenarios as depicted in Fig. 3. For the first two cases shown in Fig. 5a and 5b, the pressure doesn't reach its bound in the whole process while multistage NMPC starts decreasing the flowrate at about $t = 46$ min. Because the controller doesn't know the uncertainty in the next time step, it always selects a control input that is feasible for all three possible values of this uncertain parameter. For the third case in Fig. 5c, where the constraint violation occurs when using standard NMPC, no constraint violations occur with multistage NMPC. The controller notices that the pressure reaches its bound and then starts to decrease the flowrate to maintain the bound on pressure. Multistage NMPC can satisfy the constraints for all uncertainties included in the scenario tree.

4.2 Comparison of computational performance of different robust horizon

We now consider multistage NMPC with different robust horizons $N_r = 1$ and $N_r = 2$ and compare their tracking errors and computational time. Starting from this section and forward, we now have a problem setup where the uncertain parameter is both time-varying and randomly selected in a continuous interval (instead of a discretized finite set). For instance, one uncertain parameter in this case study is E, which can be realized randomly within $\pm 5\%$ deviation (i.e. E takes any value from $[2.28, 2.52]$ $\times 10^{10}$) instead of remaining constant in all runs.

The tracking error is calculated by averaging the sum of the difference between the control profile and the setpoint
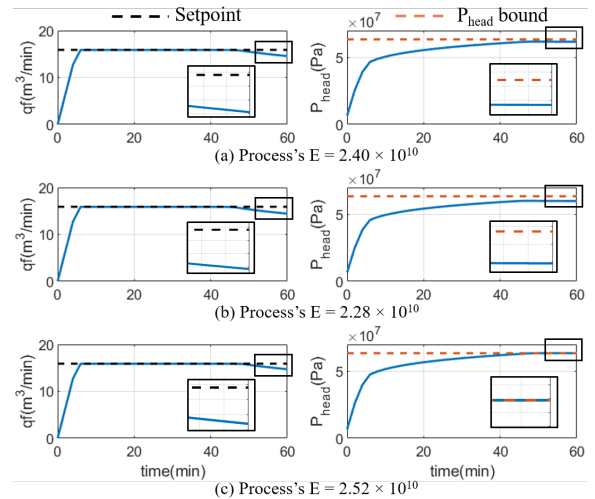
in 10 runs. The computational time is calculated also by averaging the CPU time that the solver takes to solve multistage NMPC problem in 10 runs.

Table 3. Performance comparison of different robust horizons and uncertainties

N_r and d	Tracking error(m^3/min)	CPU time(s)
$N_r = 1, \ d = E$	17.26	0.24
$N_r = 2, \ d = E$	17.31	0.77
$N_r = 1, \ d = [E, \nu]^T$	17.69	0.81

From Table 3, for cases with one uncertainty (E), the multistage NMPC with $N_r = 1$ takes less computational time than with $N_r = 2$ as expected, because the problem size for $N_r = 1$ with only 3 scenarios is smaller than the problem size for $N_r = 2$ with 9 scenarios. We also observe the tracking error results between $N_r = 1$ and $N_r = 2$ to be similar. If the uncertain parameter takes only three values (i.e. max, nominal, min), $N_r = 2$ might generate smaller tracking errors because it considers uncertainty evolution up to two stages and provides more recourse variables with more scenarios than $N_r = 1$. Instead, since our cases sample over a continuous sampling range over the uncertain parameter, having a longer robust horizon may not be as beneficial as in the discretized uncertainty case. Also, with $N_r = 2$ the degrees of freedom are restricted by the additional non-anticipativity constraints in the second prediction horizon. In other words, if we compare the same scenario in the scenario tree for $N_r = 2$ and $N_r = 1$ (e.g., maximum value of uncertainty in all stages), the former case is slightly more restricted than the latter one.

Since using $N_r = 1$ is sufficient to achieve robust performance in our case study, we recommend using $N_r = 1$ with cheaper computational effort for the rest of our simulations.

4.3 Multistage NMPC under two uncertainties

Finally, we introduce a second uncertain parameter into our hydraulic fracturing model, Poisson's ratio ν, which is another rock property in the model. Similar to Section 4.2, we also assume Poisson's ratio can vary within 5% deviation (i.e. ν takes any value from $[0.19, 0.21]$).

Both uncertain parameters, E and ν, are set to be randomly time-variant as depicted in Fig. 6a. This random realization case is controlled by multistage NMPC with $N_r = 1$ and thus 9 scenarios. From Fig. 6b and 6c, We can see that the controller still performs well even when two uncertain parameters are included in the process model, which is the more realistic case. The pressure profile oscillates slightly due to the random realization of uncertainty. The tracking error of this case is $17.69\ m^3/min$, which is larger than the other two cases in Table 3, as expected because two uncertainties are considered now. Also, the CPU time is $0.81\ s$ in this case, which is similar to the second case in Table 3 since 9 scenarios are included in both multistage NMPCs. The case with two randomly realized uncertainties is repeated for 10 runs and no constraint violation occurs, which makes us more confident to apply the multistage NMPC to cases in the real world.

(a) Random realization of two uncertainties: E & v

(b) Flowrate q_f

(c) Well head pressure P_{head}
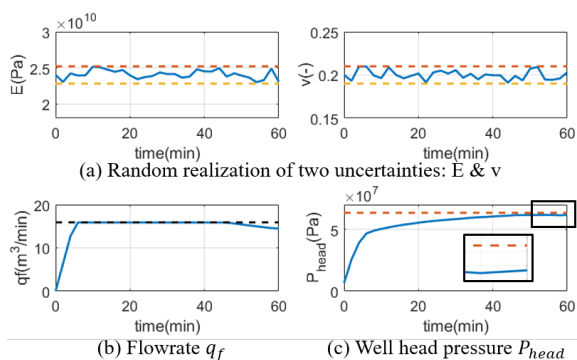
Fig. 6. Multistage NMPC with two time-variant uncertainties

5. CONCLUSIONS AND FUTURE WORK

In this work, we build a dynamic model for the hydraulic fracturing process and control the process by standard NMPC and multistage NMPC. Our results show that standard NMPC performs well when rock properties are perfectly known, but it cannot guarantee performance when there is parameter mismatch. On the other hand, multistage NMPC shows good performance with one or two time-variant or time-invariant uncertainties. We also compare computational performance for different lengths of robust horizon for multistage NMPC. Future directions will consider more control inputs to the fracturing model; this study considers only one control input (q_f). On the other hand, in real processes, both the concentration of proppant, which keeps the fracture open, and the concentration of the friction reducer must be considered. Therefore, the mass balance should be extended to these components to make the model more realistic. Additionally, at this stage we assume that all the states can be measured perfectly, while in practice only the wellhead pressure is measurable. Thus, we also need to consider on-line state estimation problems to obtain all state variables required for NMPC.

REFERENCES

Bellout, M.C., Echeverría Ciaurri, D., Durlofsky, L.J., Foss, B., and Kleppe, J. (2012). Joint optimization of oil well placement and controls. *Computational Geosciences*, 16(4), 1061–1079.

Daemen, J.J. and Schultz, R.A. (1995). *Rock Mechanics: Proceedings of the 35th US Symposium on Rock Mechanics.* CPC Press.

Detournay, E., Cheng, A.H.D., and McLennan, J.D. (1990). A Poroelastic PKN Hydraulic Fracture Model Based on an Explicit Moving Mesh Algorithm. *Journal of Energy Resources Technology*, 112(4), 224–230.

Gu, Q. and Hoo, K.A. (2015). Model-based closed-loop control of the hydraulic fracturing process. *Industrial and Engineering Chemistry Research*, 54(5), 1585–1594.

Hart, W.E., Watson, J.P., and Woodruff, D.L. (2011). Pyomo: Modeling and solving mathematical programs in Python. *Mathematical Programming Computation*, 3(3), 219–260.

Holtorf, F., Mitsos, A., and Biegler, L.T. (2019). Multistage nmpc with on-line generated scenario trees: Application to a semi-batch polymerization process. *Journal of Process Control*, 80, 167 – 179.

Jafarpour, B. and McLaughlin, D.B. (2009). Estimating channelized-reservoir permeabilities with the ensemble kalman filter: The importance of ensemble design. *Society of Petroleum Engineers*, 14(02), 374 – 388.

Kovalyshen, Y. and Detournay, E. (2010). A reexamination of the classical PKN model of hydraulic fracture. *Transport in Porous Media*, 81(2), 317–339.

Lucia, S., Finkler, T., and Engell, S. (2013). Multi-stage nonlinear model predictive control applied to a semi-batch polymerization reactor under uncertainty. *Journal of Process Control*, 23(9), 1306 – 1319.

Narasingam, A., Siddhamshetty, P., and Kwon, J.S.I. (2018). Handling spatial heterogeneity in reservoir parameters using proper orthogonal decomposition based ensemble kalman filter for model-based feedback control of hydraulic fracturing. *Industrial & Engineering Chemistry Research*, 57(11), 3977–3989.

Nordgren, R.P. (1972). Propagation of a vertical hydraulic fracture. *Society of Petroleum Engineers Journal*, 12(04), 306–314.

Perkins, T.K. and Kern, L.R. (1961). Widths of Hydraulic Fractures. *Journal of Petroleum Technology*, 13(09), 937–949.

Qin, S. and Badgwell, T.A. (2003). A survey of industrial model predictive control technology. *Control Engineering Practice*, 11(7), 733 – 764.

Siddhamshetty, P., Yang, S., and Kwon, J.S.I. (2018). Modeling of hydraulic fracturing and designing of online pumping schedules to achieve uniform proppant concentration in conventional oil reservoirs. *Computers and Chemical Engineering*, 114, 306 – 317.

Singh Sidhu, H., Siddhamshetty, P., and Kwon, J.S. (2018). Approximate dynamic programming based control of proppant concentration in hydraulic fracturing. *Mathematics*, 6(8), 132.

Waechter, A. and Biegler, L.T. (2006). On the implementation of an interior-point filter line-search algorithm for large-scale nonlinear programming. *Mathematical Programming*, 106(1), 25–57.

Yu, Z.J. and Biegler, L.T. (2019). Advanced-step multistage nonlinear model predictive control: Robustness and stability. *Journal of Process Control*, 84(20), 192–206.